UNCLASSIFIED

UNCLASSIFIED

REPORT LA 11
This is copy __3__ of __36__ copies

This document contains __40__ pages.

LOS ALAMOS HANDBOOK OF NUCLEAR PHYSICS

H. A. Bethe and R. F. Christy

Cl-------- ---- ------- ------ -----IED
by --- --- ---- --- --- ----- Commission,
Per *H. F. Carroll, Chief, Decl Br, ORdld* 2-18-65
By REPORT LIBRARY *H. Haney, 3-1-65*

UNCLASSIFIED

UNCLASSIFIED

-2-

CONTENTS

UNCLASSIFIED

1. Spontaneous fission rates

28	$5.7 \pm .5$	$\dfrac{\text{fissions}}{\text{sec Kg.}}$
25	10.5 ± 3.6	$\dfrac{\text{fissions}}{\text{sec Kg.}}$
49	< 40	$\dfrac{\text{fissions}}{\text{sec Kg.}}$

2. Impurity Limits in 49

The following impurity limits are given in parts by weight, and are based on 3000 n/sec for any one impurity in 20 Kg of 49. Strictly, it is not the fraction of the impurity that determines its effect but the total amount so that the limits are actually inversely proportional to the total mass of 49.

Li	Be	B	C	N	O	F
3×10^{-7}	1.5×10^{-7}	5.5×10^{-7}	1.2×10^{-4}	-	2.2×10^{-4}	1.5×10^{-6}

Ne	Na	Mg	Al	Si	P	S
1.5×10^{-5}	1.3×10^{-5}	1.4×10^{-5}	2.9×10^{-5}	1.3×10^{-4}	10^{-3}	7.5×10^{-3}

Cl	K	Ca	Ti	Cr	Mo	Fe
1.5×10^{-4}	7.5×10^{-4}	1.5×10^{-3}	3×10^{-3}	7.5×10^{-3}	1.5×10^{-2}	3×10^{-2}

Co	Ni
3×10^{-2}	7.5×10^{-2}

2± Energy units:

$$1 \text{ Kg} = 7.2 \times 10^{20} \text{ ergs} = 20,000 \text{ tons TNT}$$
$$1 \text{ ton TNT} = 3.6 \times 10^{16} \text{ ergs}.$$

3. Back scattering of dense elements

Element		Cross-section for elastic scattering in backward hemisphere in Barnes		Elastic back scattering per cc	
		1.5 Mev	5 Mev	1.5 Mev	5 Mev
Pb	Pb	1.63	1.05	.054	.035
Bi	Bi	1.73		.049	
Pt	Pt	.71	.48	.047	.032
W	W	.73	.47	.046	.030
Au	Au	.77	.49	.046	.029
Ta	Ta	.53	.40	.029	.022

In this table, all scattering which leaves the neutrons above the fission threshold of 28 is called elastic. The back scattering in Uranium appears to be of the same order of magnitude as in Pt, W and Au but is less certain because of a large fission correction.

4. Thermal neutron fission cross-sections

$$\sigma_f (25) = 600 \times 10^{-24} \text{ cm}^2 \text{ at } kT$$

$$\sigma_f (49) = 1200 \times 10^{-24} \text{ cm}^2 \text{ at } kT \text{ based on } \tfrac{1}{2} \text{ life} = 20,000 \text{ yrs.}$$

$$\sigma_f (23) = 1200 \times 10^{-24} \text{ cm}^2 \text{ at } kT$$

5. Number of neutrons per fission for 25

$$\nu = 2.2$$

This is based on $\eta = \dfrac{\nu \sigma_f}{\sigma_f + \sigma_c} = 1.29$ (C190)

and $\sigma_f = 4.6 \times 10^{-24} \text{ cm}^2$ and $\sigma_c = 3.2 \times 10^{-24} \text{ cm}^2$ in normal Uranium (CP257).
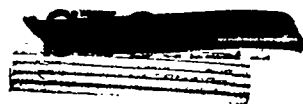
The probable error in ν is at least 10%.

6. Miscellaneous neutron cross-sections (in Barnes)

Thermal neutrons (Energy kT) $\qquad N = 2.22 \times 10^5 \, cm/sec.$

Hydrogen	$\sigma_c = .33$	$\sigma_s = 42$	L diff in $H_2O = 2.86$ cm.
Deuterium	$\sigma_c \approx .001$	$\sigma_s = 5.7$	
Graphite	$\sigma_c = .0049$	$\sigma_s = 4.8$	L diff (AGX) = 45 cm, L(AGOT) = 50 cm.
Oxygen	$\sigma_c \approx .001$	$\sigma_s = 4.1$	
Boron	$\sigma_c = 740$		
Manganese	$\sigma_c = 12.0$		
Indium	$\sigma_c = 160$		
Uranium (normal)	$\sigma_c = 3.0$	$\sigma_s = 12$	
	$\sigma_f = 4.3$		
	$\sigma_a = 7.3$		

Cd . $\qquad \sigma_a = 2800$

see also CP333 $\qquad$ CP729.

Fast neutrons $\qquad$ see CP334 $\qquad$ CF458.

7. Calibration of slow neutron detectors

1. Indium Foils

The standard foil at Chicago is 4×6.5 cm^2, 5 mils thick and weighs 2.4 gm. The standard Cd covering is 20 mils thick. If the activities A are measured in counts per minute at saturation on standard thin wall counters then the thermal neutron flux $nv = .102 \, A_{th}/(cm^2 \, sec)$ where $A_{th} = (A - 1.07 \, A_{cd})$. Here A_{cd} is the activity of the foil when covered with cadmium and A is the activity of the uncovered foil.

also $q_{In} = .00143 \, A_{cd}$ where q_{In} is the number of neutrons per cc crossing In resonance energy per sec.

2. Manganese Dioxide Foils

$$nv = .80 \, (A/gm) / (cm^3 . sec)$$
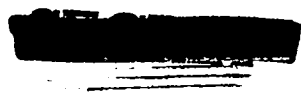
8. Calibration of fast neutron detectors

1. Hydrogen-containing gas

For neutrons traversing a chamber of methane at atmospheric pressure (20 C.), the following table gives the probability of a proton recoil <u>per cm of path</u> of the neutron. The second line gives <u>all</u> recoils, the last only the recoil protons of energy greater than .5 Mev.

Energy (Mev)	0.2	0.5	1	1.5	2	3	5
Probability of recoil	10	6.2	4.3	3.5	3	2.3	1.5×10^{-4}
Recoils over .5 Mev	-	0	2.2	2.3	2.2	1.9	1.35×10^{-4}

The probability of a recoil (detection efficiency) is proportional to the gas pressure and to the number of hydrogen atoms per molecule.

2. Thin paraffin

For neutrons traversing at right angles a layer which is thin compared to the range of the protons, 1 mg/cm^2 of paraffin is equivalent to 0.89 cm of methane at atmospheric pressure (case 1).

3. Thick paraffin

For neutrons incident normal to a paraffin slab of which the thickness is larger than the range of the fastest recoils, the following table gives the total number of protons emerging from (one side of) the paraffin per incident neutron.

Neutron energy	0.2	0.5	1	1.5	2	3	5	Mev
Efficiency of detection			2.4	3.7	5.2	7.8	12.5×10^{-4}	

4. Fast Fission

A detector of 28, of thickness 1 mg/cm^2, with neutrons incident on it at right angles has an efficiency $\underline{1.7 \times 10^{-6}}$

5. Induced radioactivity

Efficiency 10^{-5} to 10^{-3}
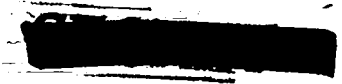
9. Scattering cross-sections of Carbon, Oxygen, Deuterium

These curves are based on reliable measurements taken by Williams with the Van de Graaf at Minnesota. (CF599 and CF507)

10. Scattering cross-section of Hydrogen

This curve is a copy of that by Bohm and Richman. It is based on a square potential hole with a square tail which fits best the measurements of Williams (CF599).
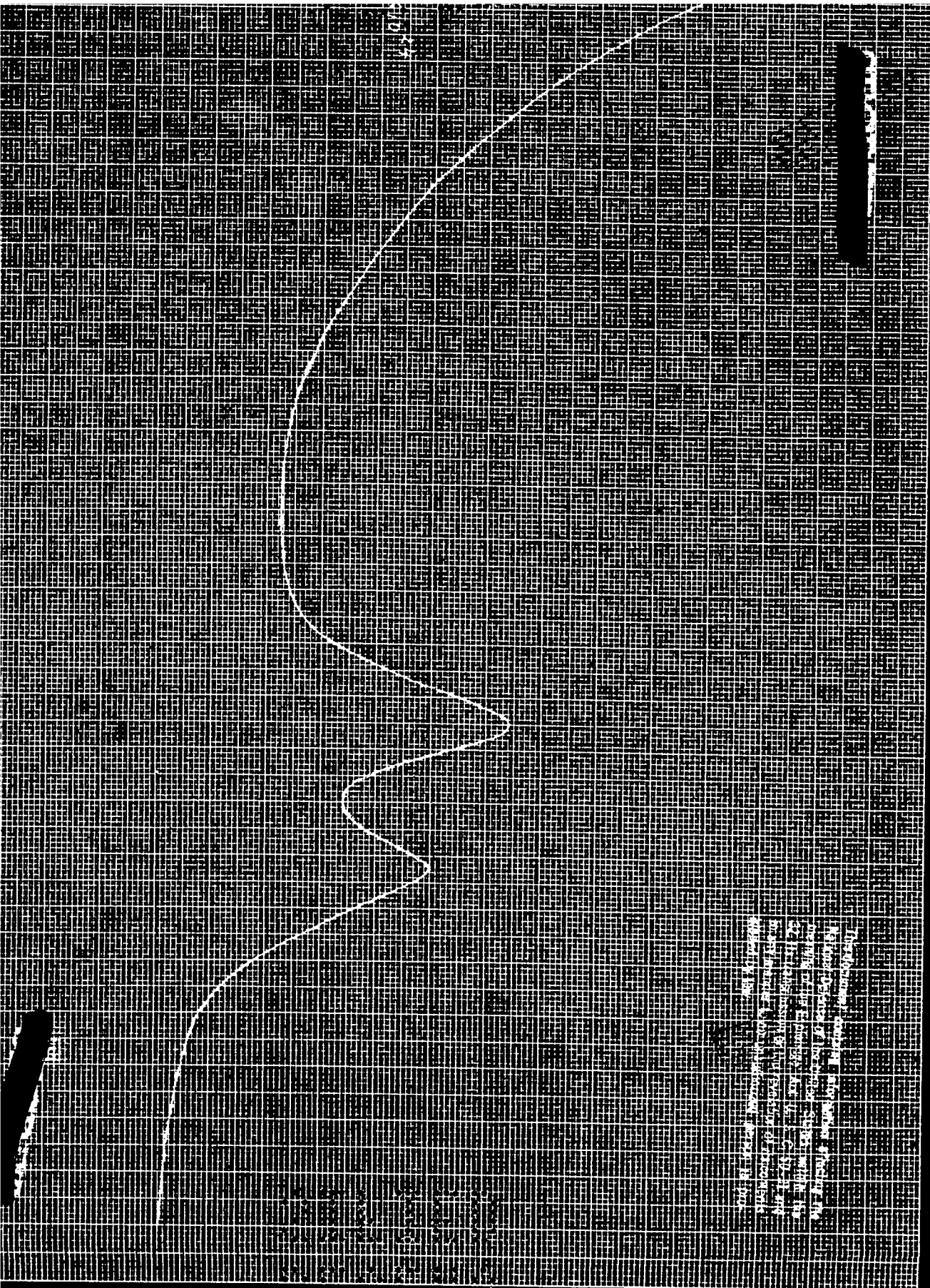
11. Fission cross-sections of 25, 28 and 49

The curve for σ_f (25) is due to Hanson (CF618) and is considered reliable for relative values. Two absolute scales are given: one from the coincidence counter calibration of Hanson (CF618) and the other from Manganese bath comparison with Chicago standard sources by Hanson (CF638) and by Heydenburg (CF636). The two scales are given to emphasize the present unreliability of the absolute values. Segre's points (CF403) are not included because of doubt of the energy values. These two scales introduce a distortion of the σ_f (28) curve since the low energy ($<$ 2 Mev) points were measured according to the first scale (CF618) and high energy points by the second (CF636). The shape of curve so drawn seems inconsistent with the low energy points. The σ_f (49) curve is based on relative values of $\dfrac{\sigma_f (49)}{\sigma_f (25)}$ obtained at L. A. up to 1 Mev. The curve is continued above 1 Mev by means of a high energy point by Heydenburg (CF626). $\dfrac{\sigma_f (49)}{\sigma_f (25)}$ (thermal) is taken to be 2.00.

12. Angular distribution of scattering in Uranium

The scattering from 90° to 180° was obtained from measurements on back scattering at Wisconsin (CF625). That from 0° to 90° was obtained from measurements at Minnesota of $\int_{\Theta}^{180°} \sigma_s \, d(\cos \Theta)$ with $\Theta = 30°$, 60°, 90°, and from measurements of the total cross-section. These results will be somewhat changed by more accurate evaluation of corrections.

13. Cross-sections of Uranium

The total cross-section was measured at Minnesota (CF507). The elastic and inelastic scattering cross-sections were obtained from the preceding measurements together with σ total and σ fission. The transport cross-section was also obtained from the angular distribution curves and includes inelastic scattering and fission. The usual definition of inelastic cross-section (scattering to below the fission threshold) breaks down below 1 Mev, a smooth curve was drawn in this region to indicate the lack of any real discontinuity. These results will also be somewhat changed by re-evaluation of the corrections.

14. The fission spectrum

The fission spectrum is that reported by Bloch (CF525) with the more recent energy calibration which reduces all energies to 3/4 of their value. The spectrum is normalized to $\bar{\nu} = 2.2$.

Scattering cross-section of Uranium at ~1Mev   (per unit cos θ)

$\sigma = x \cdot 10^{-24} cm^2$

9
8
7
6
5
4
3
2
1

-1.0 -.9 -.8 -.7 -.6 -.5 -.4 -.3 -.2 -.1 0 .1 .2 .3 .4 .5 .6 .7 .8 .9 1.0

Cos θ

90°   60°   30°

Scattering Cross-section of Uranium at ~3 Mev (per unit cos θ)
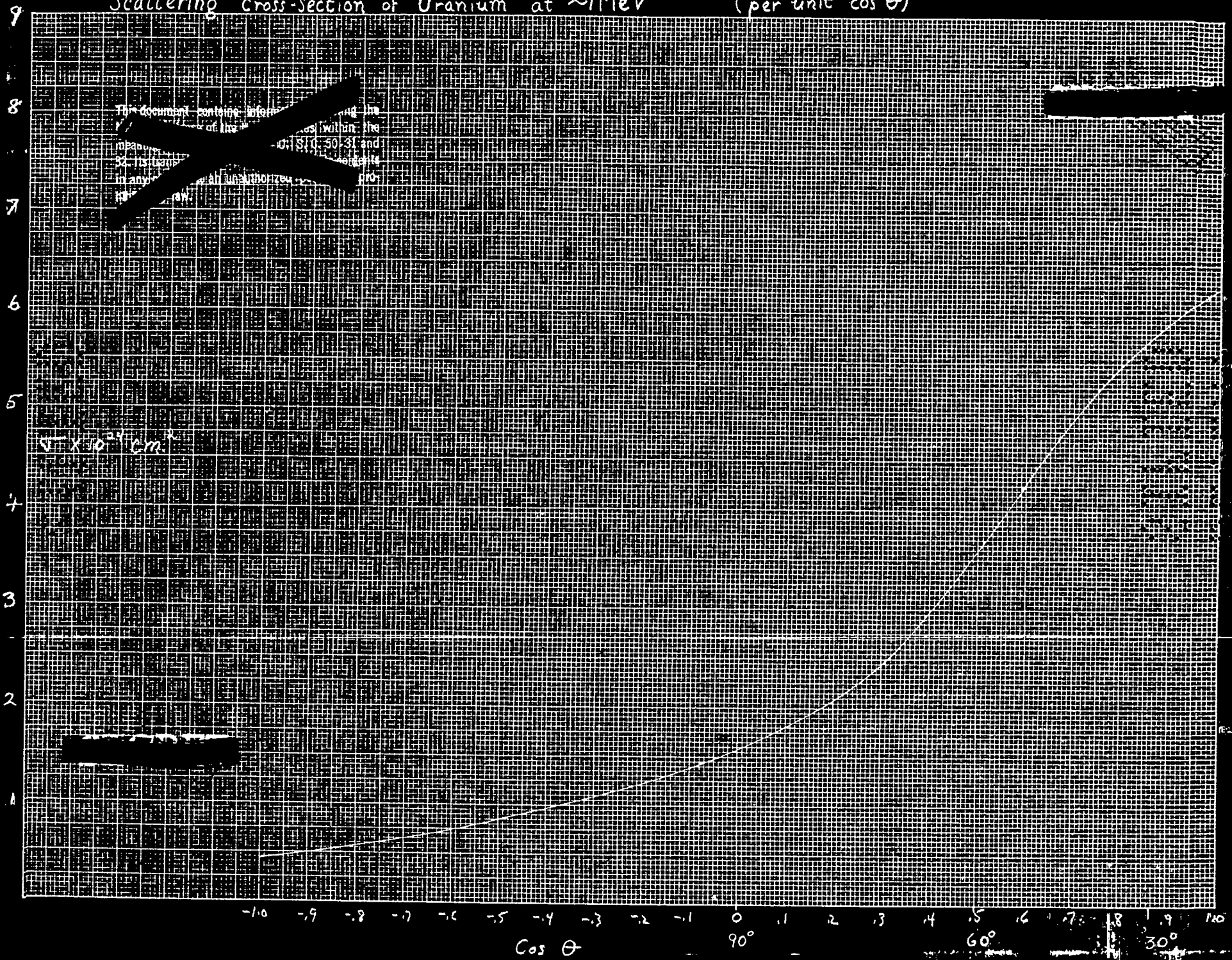
This document contains information affecting the ... the United States ...
meaning or ... and
32. Its transmission ... contents
in any man... unauthorized
hibi...
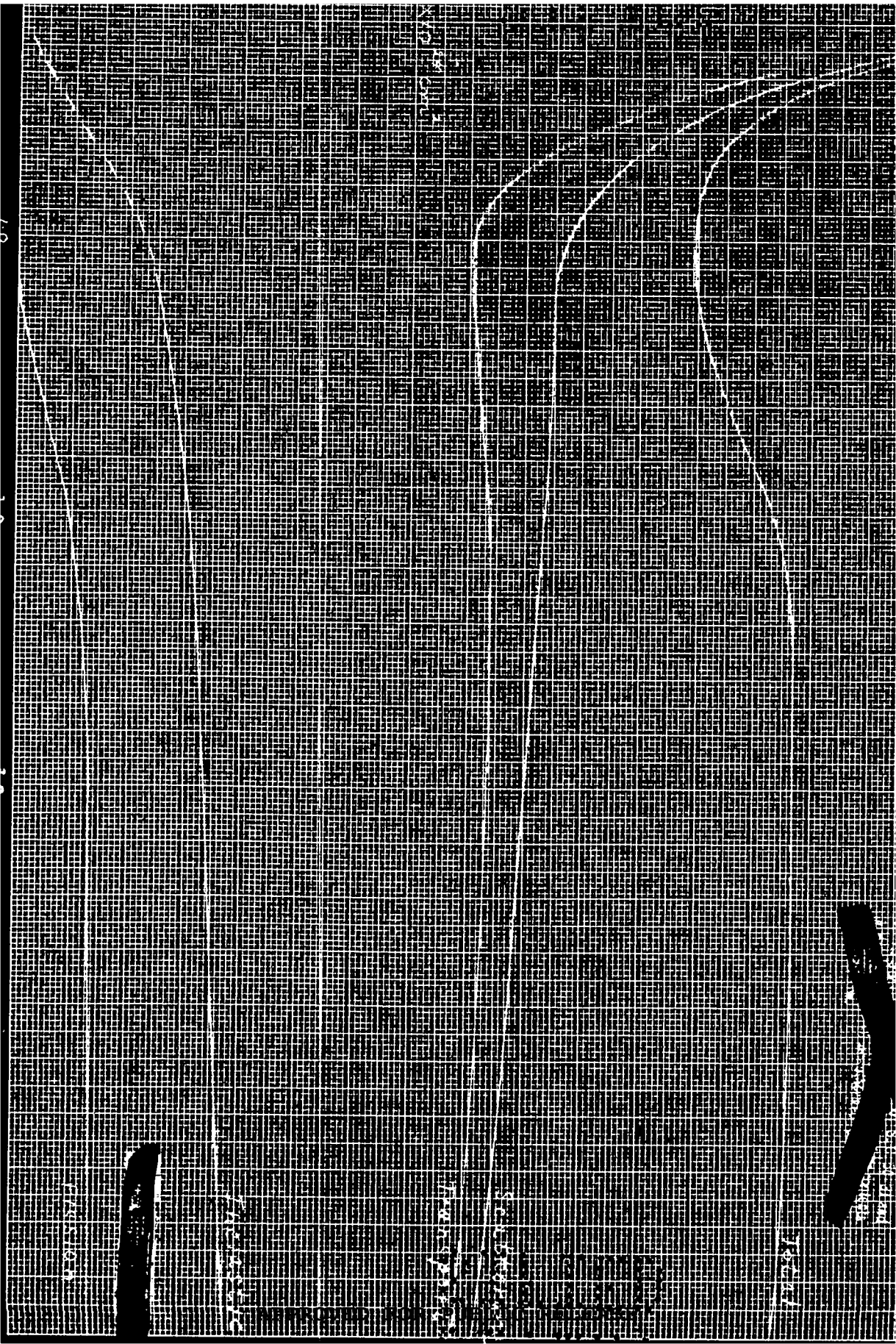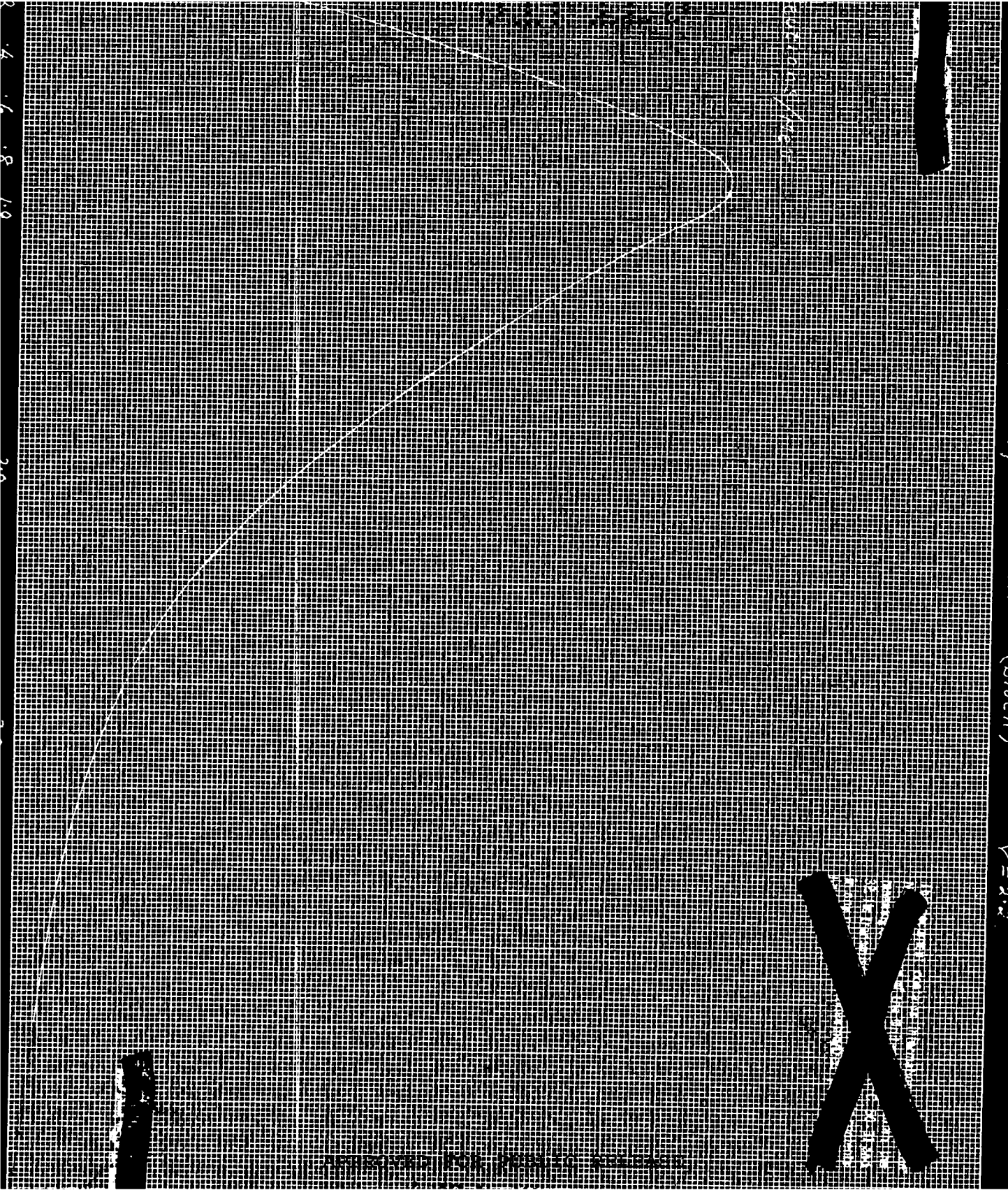
15. The Carbon d-n source

The shape of the thin target yield (cross-section) curve and of the thick target yield curve was obtained from thin target measurements at Rice (Phys. Rev. 58,185, 1940) and Minnesota (Phys. Rev. 60,80, 1941). The absolute value of the thick target yield at 875 Kev was obtained from a calibration by Heydenburg (CF604). This gave absolute values for both curves.

16. The D_2O-ice d-n source

The angular distribution curve was measured at Rice (CF350). The other curves (thin and thick target yields) were obtained from a relative thin target curve for $E_d > .5$ Mev at Rice (CF350), an absolute thick target curve for $E_d < .3$ Mev at Chicago, and an absolute measurement for a thick target by Heydenburg (CF604) at 900 Kev.

17. Neutron yield from Li-p-n reaction

The curve is based on measurements of Hanson with a Wisconsin Van de Graaf generator. It gives the yield per microcoulomb of proton current, per $\frac{mg}{cm^2}$ of lithium target, and per unit solid angle in the forward direction. The following conversion factors may be used:

$1 \frac{mg}{cm^2}$ of Li $= 1.04 \frac{mg}{cm^2}$ of air equivalent

$= 164$ kv stopping power at the reaction threshold (1.8 Mev)

Cross-section (for solid angle of 4π) in barns

$= .235 \times 10^{-7}$ x yield given in curve.

Angular distribution $I + A \cos^2 \theta$ in C.G. system for $D(d,n)$ reaction
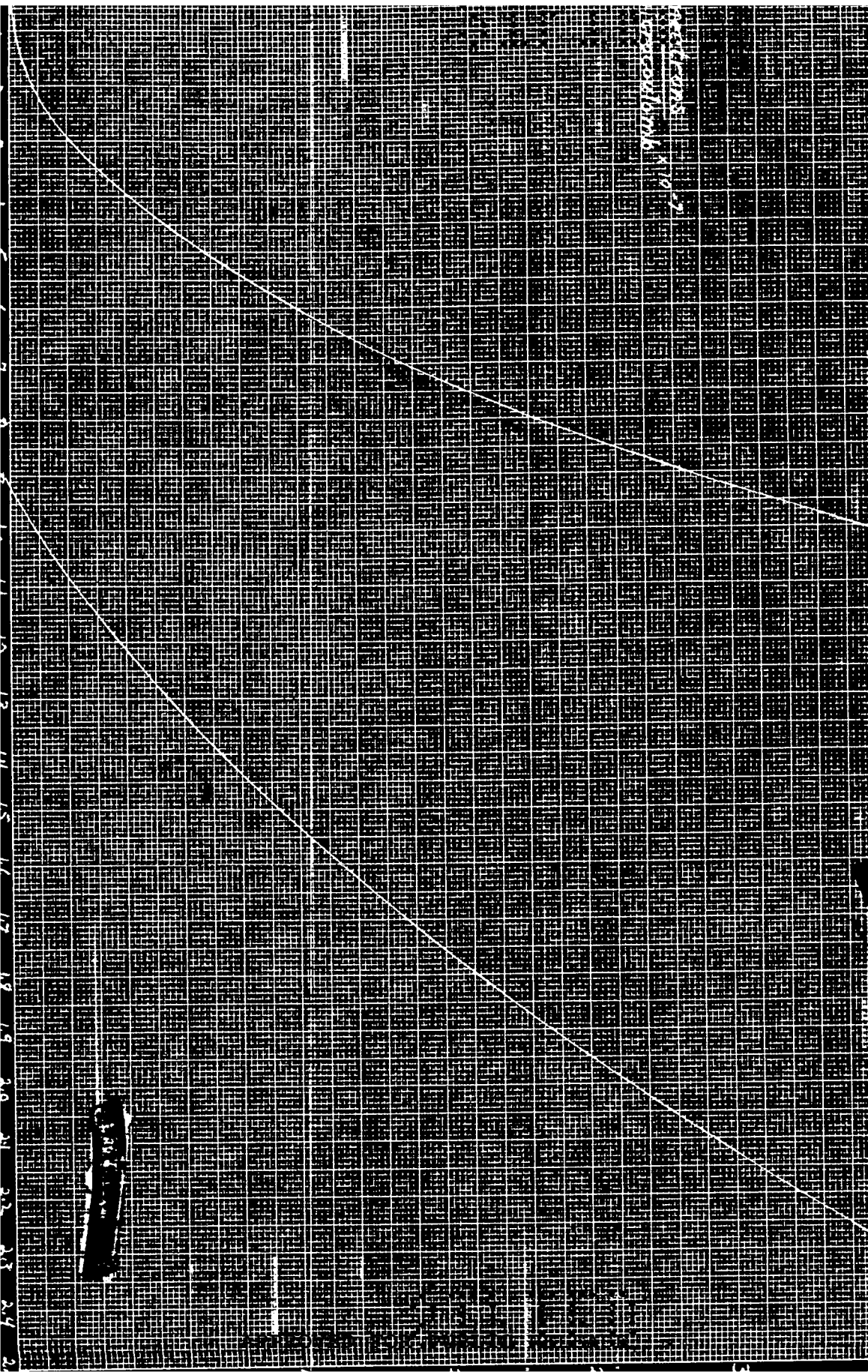
Thin target neutron yield
per microcoulomb per mg/cm²
of Li per unit solid
angle in e forward direction

$En = \frac{3}{4} Ep + \frac{1}{32} Ep \cos^2\Theta - 1.42 + \frac{1}{4}\sqrt{\frac{3}{4} Ep + \frac{1}{64} Ep \cos^2\vartheta - 1.42}\ \sqrt{Ep}\ \cos\vartheta$

$En(\vartheta) \approx En\left(\frac{\pi}{2}\right) + \frac{\sqrt{Ep}}{4}\sqrt{En\left(\frac{\pi}{2}\right)}\ \cos\vartheta$

$\theta = 0°$

$\theta = \frac{\pi}{2}$

$$E_n = \frac{11}{14} E_D + \frac{1}{49} E_D \cos^2\theta + \frac{13}{14} Q + \frac{1}{7} \sqrt{2 \left(\frac{11}{14} E_D + \frac{1}{98} E_D \cos^2\theta + \frac{13}{14} Q \right)} \sqrt{E_D} \cos\theta$$

$$Q = -0.27 \ MV$$
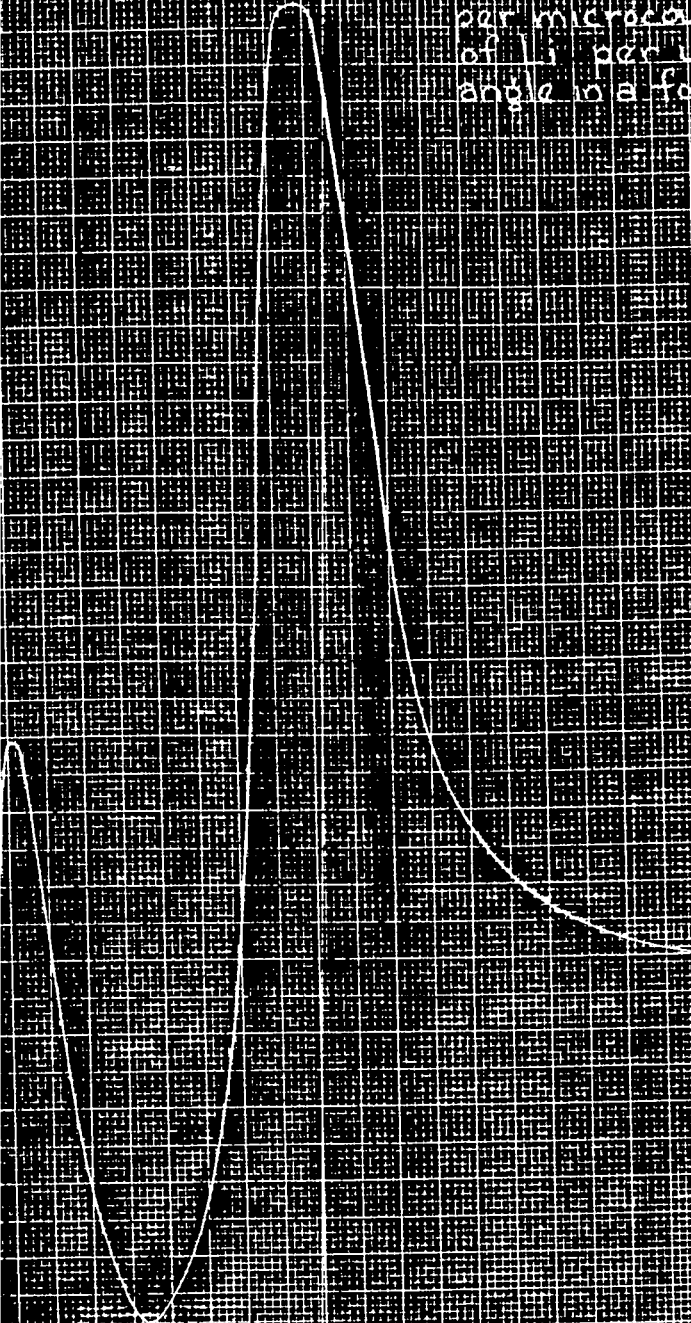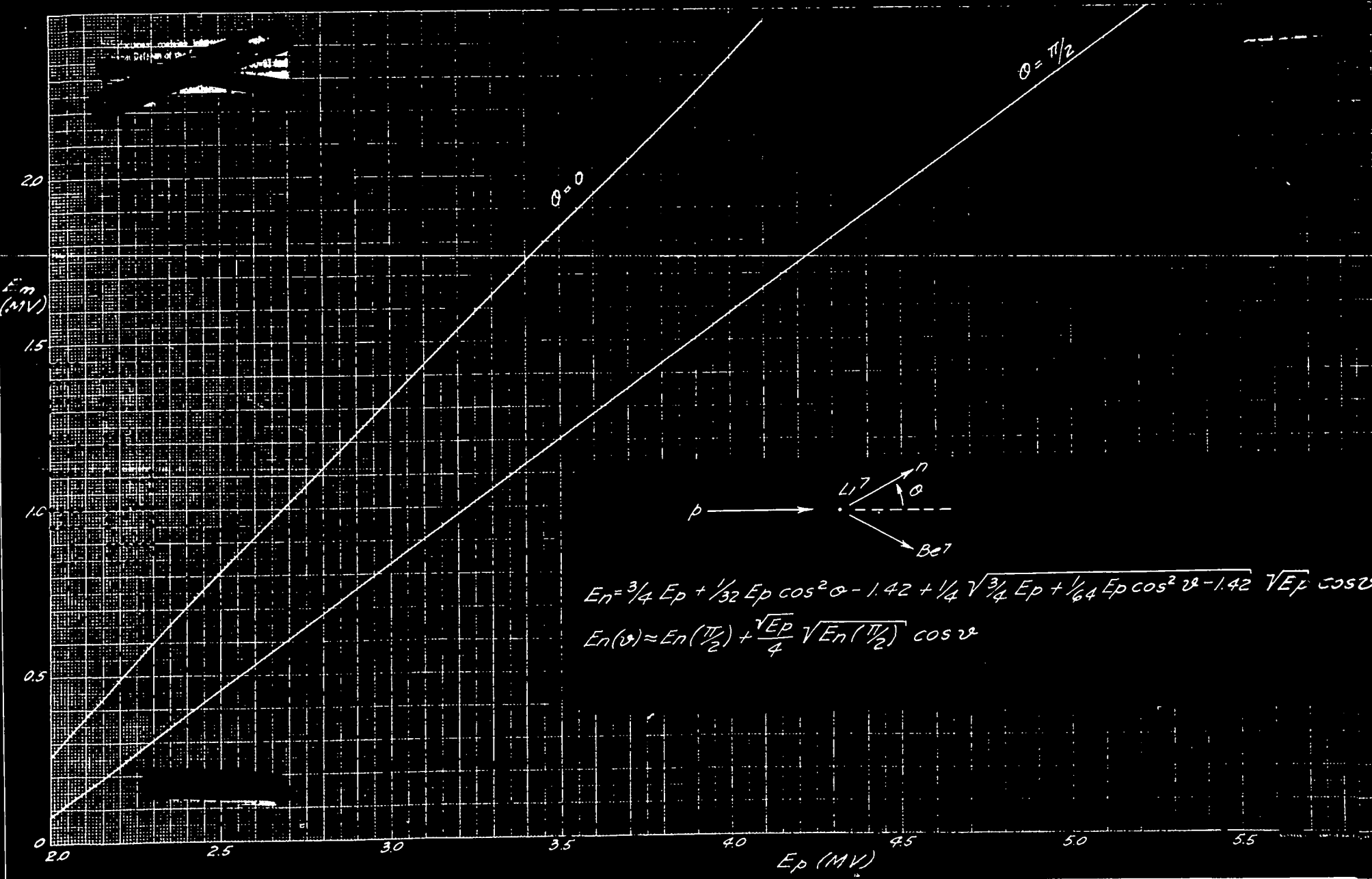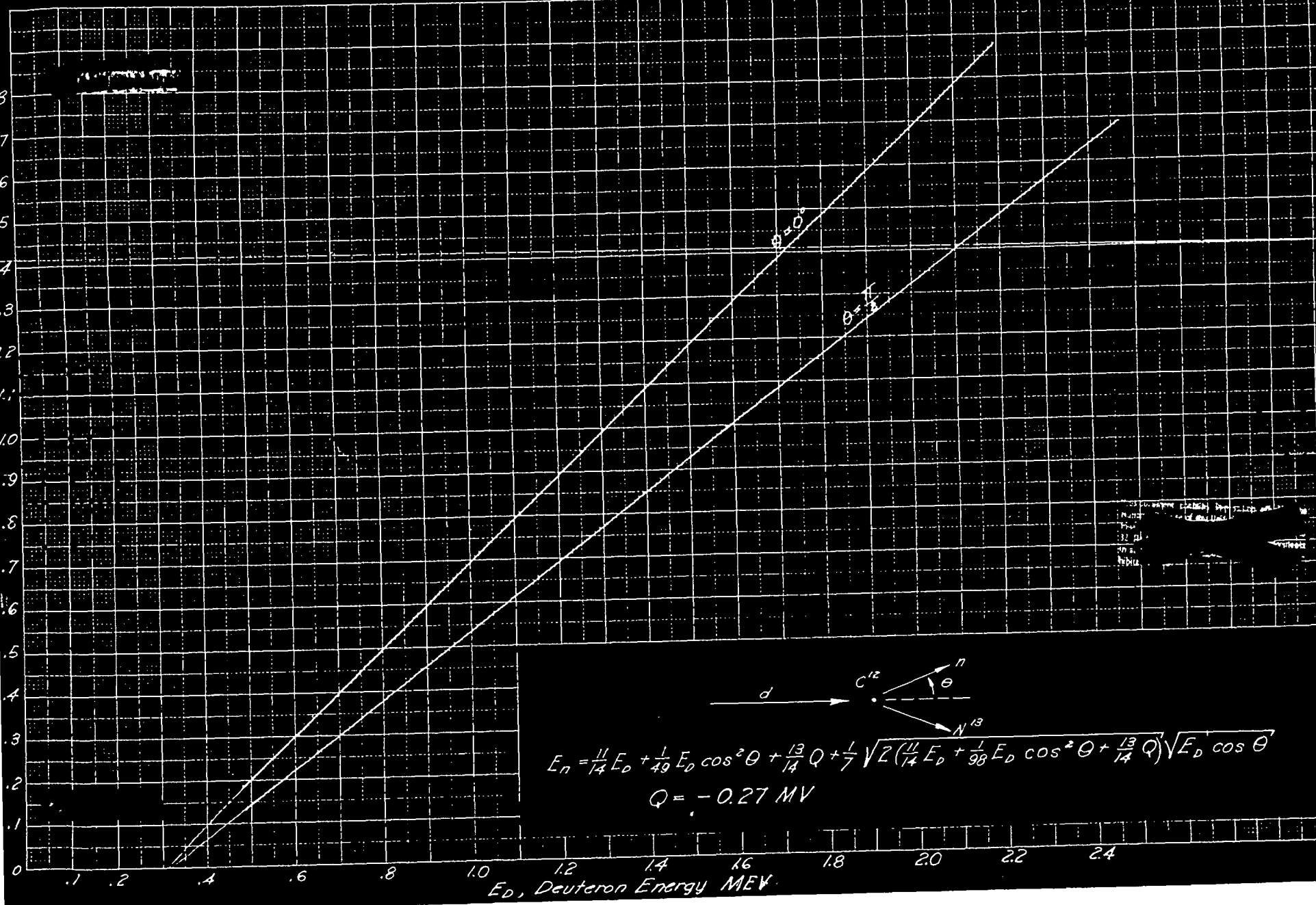
E_D, Deuteron Energy MEV

$$E_n = \frac{1}{4} E_d (1 + \cos^2 \Theta) + 2.48 + \frac{\sqrt{E_d}}{4} \sqrt{E_d(2 + \cos^2 \Theta) + 19.86 \; \cos}$$
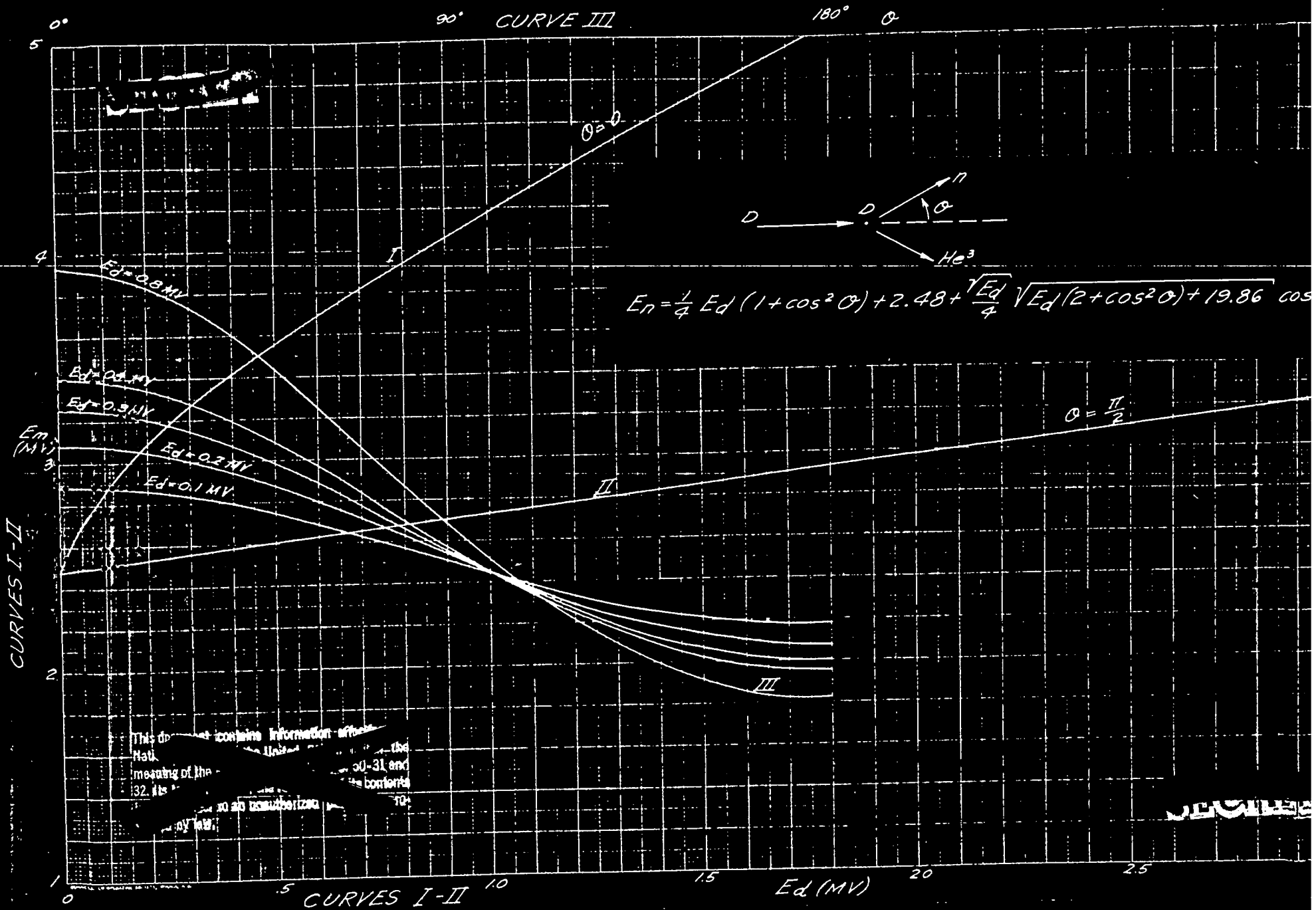
18. Range-energy relations

For fast α-particles and protons the curves in the article by Livingston and Bethe in the Reviews of Modern Physics may be used. The curve given here for slow α-particles is based on measurements by Holloway and Livingston, Phys. Rev. 54, 18 (1938). The curve for slow protons in air is a re-evaluation of the experiments of Parkinson, Herb, Bellamy and Hudson, Phys. Rev. 52, 75 (1937).

The range-energy relation for deuterons in (heavy) water was calculated by Ashkin on a purely theoretical basis. The theoretical stopping power for oxygen which was used in these calculations was compared with the experimental data for air and found to be in satisfactory agreement (about 3 percent difference after correcting for the different nuclear charge). These calculations together with curves for the stopping power of H_2 and O_2 will be published in Los Alamos Report #12 by Ashkin.

Energy vs. Range
Protons and Deuterons

Mean Range ~15°C and 760 mm

Cornell University
1937
Revised

○ - Parkinson, Herb, Bellamy, and Hudson

Energy vs. Range
α Particles
Mean Range – 15°C and 760 mm.

Cornell University
1938
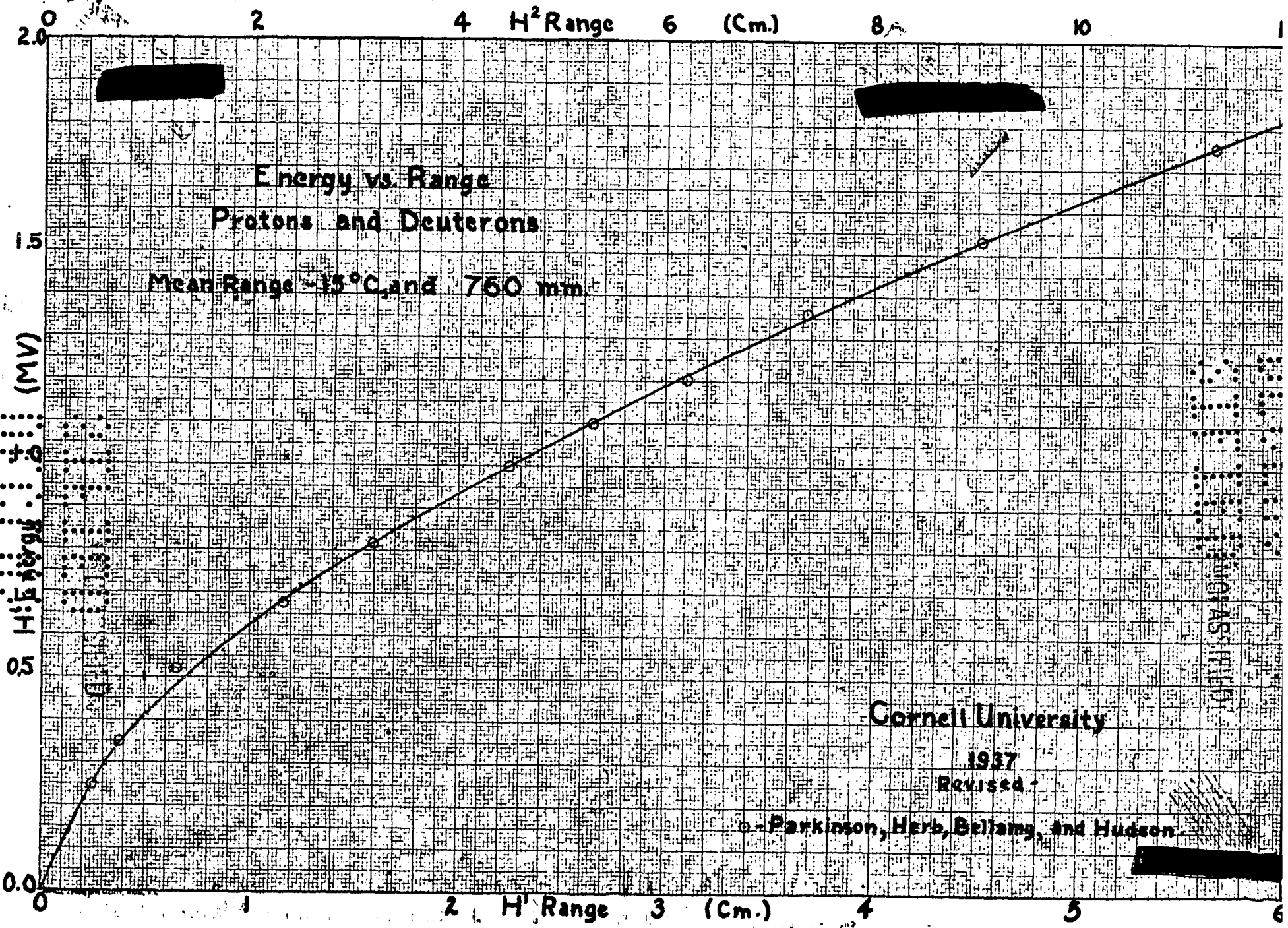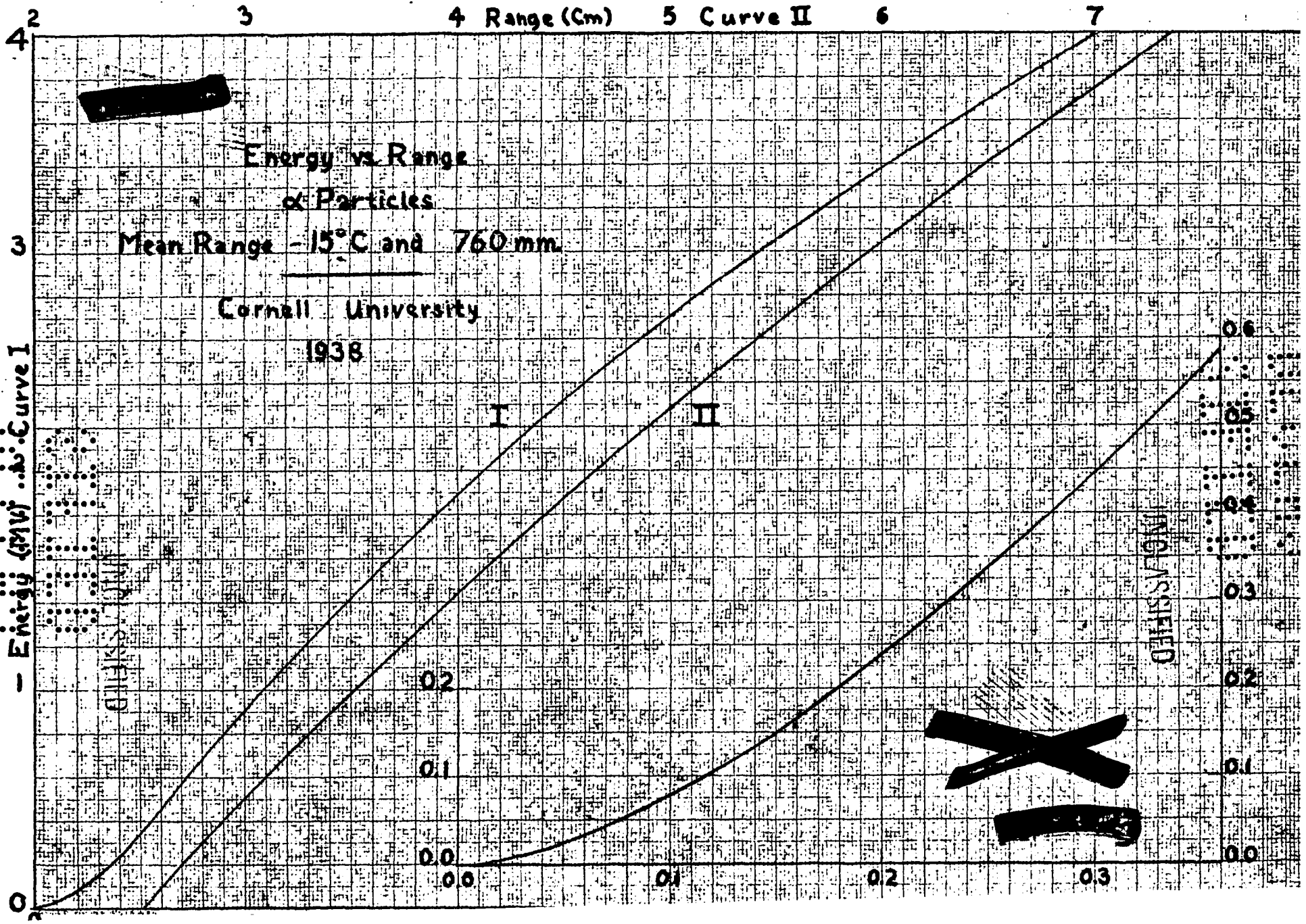
19. Isotopic masses and abundance.

This table contains the isotopic mass values which we consider most reliable. As can be seen from the given "probable errors", the masses up to neon are very much more accurately known than for the heavier elements. The lighter masses were calculated taking into account all of the more accurate data from mass spectrograph as well as disintegrations and attempting the best possible fit.

Abbreviations used in the isotopic mass table:

Abundance: For stable isotopes, the abundance is given in percent. Radioactive elements are indicated by the particle they emit ($\beta-$ or $\beta+$); βc means that the nucleus captures an orbital electron but does not emit positrons. P means instability against disintegration into heavy nuclear particles.

Mass values in parenthesis refer to nuclei which have not yet been produced.

The errors listed are meant to be about 3 times the probable or twice the "standard" error. For theoretical estimates, the "error" is usually not given.

Sources of the data are indicated as follows:

I = calculations by Betty J. Isaacs, Cornell University, Master's Thesis, 1942

W Wigner, Memorandum #24, April 2, 1940.

B = Barkas, Phys. Rev. 55, 691 (1939)

M = Mass spectrograph value (usually most reliable)

D = from Disintegration Experiments involving heavy particles

   from end point of β-spectrum

C = calculated value

corr = corrected in view of more recent accurate determination of the mass of

   a neighboring isotope from which the mass of the given isotope is obtained through a disintegration measurement or a theoretical estimate

E = estimate

Z	Element	A	Abundance percent	Mass	Error x 10⁵	Source
0	N	1	β -	1.00893	3	ID
1	H	1	99.98	1.008123	0.6	IM
1	H	2	.02	2.014708	1.1	IM
1	H	3	β -	3.01702	3.4	ID
2	He	3	10⁻⁵	3.01700	4	Iβ
2	He	4	100	4.00390	3	IM and D
2	He	5	P	5.0137	35	ID
2	He	6	β -	6.0209	50	Iβ
3	Li	5	P	(5.0136)	(60)	WC
3	Li	6	7.9	6.01697	5	ID
3	Li	7	92.1	7.01822	6	IM and D
3	Li	8	β -	8.02502	7	D
4	Be	6	β +	6.0219	(100)	WC
4	Be	7	βc	7.01916	7	ID
4	Be	8	P	8.00785	7	ID
4	Be	9	100	9.01503	6	ID
4	Be	10	β -	10.01677	8	ID
4	Be	11	P	(11.0277)	-	WC
5	B	9	P	9.01620	7	ID
5	B	10	18.4	10.01618	9	IM and D
5	B	11	81.6	11.01284	8	IM and D
5	B	12	β -	12.0190	70	ID
5	B	13	β -	(13.0207)	-	WC
6	C	10	β +	10.0210	30	ID
6	C	11	β +	11.01495	9	ID
6	C	12	98.9	12.00382	4	IM

Z	Element	A	Abundance percent	Mass	Error ×10⁵	Source
6	C	13	1.1	13.00751	10	IM and D
6	C	14	β −	14.00767	5	ID and R
6	C	15	β −	(15.0165)	−	WC
7	N	12	(β +)	(12.0233)	−	WC
7	N	13	β +	13.00988	7	ID
7	N	14	99.62	14.00751	4	IM
7	N	15	0.38	15.00489	21	IM
7	N	16	β −	(> 16.0065) (< 16.011)	−	ID
7	N	17	β −	(17.014)	−	WC
8	O	14	β +	(14.0131)	−	WC
8	O	15	β +	15.0078	40	Iβ
8	O	16	99.76	16.000000	−	Standard
8	O	17	0.04	17.00450	6	ID
8	O	18	0.20	18.0049	40	WM
8	O	19	(β −)	19.0139)	−	WC
9	F	16	β +	(16.0175)	−	WC
9	F	17	β +	17.0075	30	ID
9	F	18	β +	18.0065	60	WD
9	F	19	100	19.00450	26	IM
9	F	20	β −	> 20.0042 < 20.0092	− −	Iβ ID
9	F	21	β −	(21.0059)	−	WC
10	Ne	18	β +	(18.0114)	−	WC
10	Ne	19	β +	19.00781	20	Wβ
10	Ne	20	90.0	19.99877	10	IM
10	Ne	21	0.27	20.99963	22	IM
10	Ne	22	9.73	21.99844	55	IM
10	Ne	23	β −	(23.0013)	−	WC

Z	Element	A	Abundance percent	Mass	Error ± .05	Source
11	Na	21	$\beta+$	(21.0035)	-	WC
11	Na	22	$\beta+$	21.9999	50	Iβ
11	Na	23	100	22.99618	31	ID
11	Na	24	$\beta-$	23.9975	45	ID
11	Na	25	$\beta-$	(24.9967)	-	WC
12	Mg	22	$\beta+$	(22.0062)	-	WC
12	Mg	23	$\beta+$	23.0002	40	Wβ
12	Mg	24	77.4	23.9924	60	Bβ
12	Mg	25	11.5	24.9938	90	WD
12	Mg	26	11.1	25.9898	50	WD
12	Mg	27	$\beta-$	26.9928	150	Wβ
13	Al	25	$\beta+$	24.9981	100	Wβ
13	Al	26	$\beta+$	25.9929	150	Wβ
13	Al	27	100	26.9899	80	WD
13	Al	28	$\beta-$	27.9903	70	Wβ
13	Al	29	$\beta-$	28.9893	80	Wβ
13	Al	30	$\beta-$	(29.9954)	-	WC
14	Si	27	$\beta+$	26.9949	90	Iβ
14	Si	28	89.6	27.9866	60	WM
14	Si	29	6.2	28.9866	60	WM
14	Si	30	4.2	29.9832	90	WD
14	Si	31	$\beta-$	30.9862	60	Wβ
14	Si	32	$\beta-$	(31.9849)	-	WC
15	P	29	$\beta+$	(28.9919)	(100)	WC
15	P	30	$\beta+$	29.9873	100	Iβ
15	P	31	100	30.9843	50	WM
15	P	32	$\beta-$	31.9827	40	Iβ
15	P	33	$\beta-$	(32.9826)	-	WC

Z	Element	A	Abundance percent	Mass	Error ±10⁵	Source
16	S	31	β+	(30.9899)	–	C
16	S	32	95.0	31.98089	7	IM
16	S	33	0.74	32.9800	60	W corr
16	S	34	4.2	33.97710	35	IM
16	S	35	β–	34.9788	80	W corr
16	S	36	0.016	35.978	100	W
17	Cl	33	β+	(32.9860)	–	WC corr
17	Cl	34	β+	33.9801	–	IB
17	Cl	35	75.4	34.97867	21	IM
17	Cl	36	βc	35.9788	100	W
17	Cl	37	24.6	36.97750	14	IM
17	Cl	38	β–	37.981	300	W
17	Cl	39	β–	(38.9794)	–	WC
18	A	35	β+	(34.9850)	–	C
18	A	36	0.307	35.9780	100	W
18	A	37	βc	(36.9777)	–	E
18	A	38	0.061	37.974	250	ID
18	A	39	β–	(38.9755)		WC
18	A	40	99.63	39.9756	60	IM
18	A	41	β–	40.9770	60	W
19	K	37	β+	(36.9830)	–	WC
19	K	38	β+	(37.9795)	–	WC
19	K	39	93.3	(38.9747)	–	WC
19	K	40	0.012	39.9760	100	W
20	Ca	40	96.96	39.9753	150	E
20	Ca	42	0.64	41.9711	–	W
20	Ca	43	0.15	42.9723		W
20	Ca	44	2.06	–		–
20	Ca	45	β–	44.968		C

Z	Element	A	Abundance percent	Mass	Error $\times 10^5$	Source
21	Sc	45	100	44.9669	–	ID
22	Ti	46	–	45.9661	100	IM
22	Ti	47	–	46.9647	100	IM
22	Ti	48	–	47.9631	50	IM
22	Ti	49	–	48.9646	60	IM
22	Ti	50	–	49.9621	40	IM
22	Ti	51	–	50.9587	100	W corr
23	V	51	–	50.9577	50	–
24	Cr	51	β c	50.958	–	W corr
24	Cr	52	81.6	51.956	–	W corr
24	Cr	53	10.4	52.956	–	W corr
25	Mn	55	100	54.957	–	E
26	Fe	54	6.04	53.957	–	W corr
26	Fe	56	91.57	55.9568	170	IM
26	Fe	57	2.11	56.957	–	W corr
26	Fe	58	0.28	–	–	–

R. P. Feynman

RESULTS

	0.6 Mev.		σ_{inel}			1.5 Mev.		σ_{inel}		
	σ_T	σ_{Back}	Total	<.1	ℓ	σ_T	σ_{Back}	Total	<.4	ℓ
U_{28}	5.16	3.8	.70	0	4.0	4.3	4.2	1.8	0.7	4.85
Pb	4.70	4.0	0	0	6.4	3.37	3.2	0.4	0	9.0
W	4.50	3.6	.80	0	4.3	4.2	3.2	1.7	0.7	4.65
Fe	1.7	1.2	.20	0	7.5 10.5	2.18	1.9	0.6	0	5.8 6.6
BeO	5.0	3.9	0	0	3.0	2.9	2.2	0	0	5.1
C	2.5	2.0	0	0	5.0	1.41	1.2	0	0	8.9
WC	7.0				3.2	5.61				4.0